Oct 17th, 12:00 AM

Determination of Purlin R-factors Using a Non-linear Analysis

Catherine J. Rousch

Gregory J. Hancock

Thirteenth International Specialty Conference on Cold-Formed Steel Structures
St. Louis, Missouri U.S.A., October 17-18, 1996

DETERMINATION OF PURLIN R-FACTORS USING A NON-LINEAR ANALYSIS

Catherine J. Rousch * Gregory J. Hancock †

SUMMARY

In both Australia and the U.S.A., the design procedure for purlins under wind uplift loading is based on the use of reduction factors (R-factors), which allow for the flexural-torsional or non-linear twisting behaviour of purlins with screw-fastened sheeting. To date, all R-factors have been determined by testing. However, in the future it may be more efficient to obtain R-factors from numerical models to minimise testing.

This paper shows how a numerical model of the twisting behaviour of channel and Z-section purlins can be used to generate R-factors. Comparisons between experimentally determined and numerically based R-factors are made.

1 INTRODUCTION

Roof and wall systems used throughout the world often consist of cold-formed steel channel or Z-section purlins screw-fastened to high tensile profiled steel sheeting. In Australia, the design of such systems is in accordance with the Australian *Cold-Formed Steel Structures Code*, AS 1538 (Standards Association of Australia, 1988), and is usually governed by wind uplift loading. A limit state version of this code, the Australian/New Zealand *Cold-Formed Steel Structures Standard* (Standards Australia/Standards New Zealand, 1996), is currently under development. In this amended draft standard, the design procedure for purlins under wind uplift loading is based on the use of reduction factors (R-factors), which allow for the flexural-torsional or non-linear twisting behaviour of purlins with screw-fastened sheeting. The R-factors in the draft standard were determined by Johnston and Hancock (1994) for simple channel and simple Z-section purlins commonly used for roof and wall systems in Australia, including the sheeting, screw-fasteners, cleats and lap lengths peculiar to Australia. The American Iron and Steel Institute (AISI) Specification (1991a), on which the draft Australian/New Zealand standard is based, also uses R-factors. However, these R-factors have been calculated for purlin-sheeting systems peculiar to the U.S.A., and are generally lower than those given in the draft Australian/New Zealand standard.

*PhD Research Student, Centre for Advanced Structural Engineering, School of Civil and Mining Engineering, The University of Sydney NSW 2006 Australia

†BHP Steel Professor of Steel Structures, Centre for Advanced Structural Engineering, School of Civil and Mining Engineering, The University of Sydney NSW 2006 Australia

To date, all R-factors have been determined from testing. However, in the future it may be more efficient to obtain R-factors from numerical models to minimise testing. A non-linear, out-of-plane elastic analysis, developed at the University of Sydney by Rousch and Hancock (1994a, 1994b), has been used to predict the failure loads and failure modes of roof and wall systems composed of simply-supported and continuous cold-formed steel channel and Z-section purlins under wind uplift loading. From the predicted failure loads, R-factors have been calculated. R-factors have also been determined from tests performed in a vacuum test rig at the Centre for Advanced Structural Engineering (1989, 1990, 1994) within the University of Sydney, the results of which have been published in Hancock *et al* (1990, 1993). In this paper, comparisons between the experimentally determined and numerically based R-factors are made.

2 NON-LINEAR ANALYSIS MODEL

A non-linear, out-of-plane elastic analysis, developed at the University of Sydney by Rousch and Hancock (1994a, 1994b), can be used to predict the failure loads and failure modes of simply-supported and continuous cold-formed simple channel and simple Z-section purlins screw-fastened to sheeting, and subject to wind uplift loading. The analysis incorporates a distorted purlin section model which is based on a combination of models developed by Peköz and Soroushian (1982), and Thomasson (1988).

2.1 Distorted Section Model

Screw-fastened systems usually provide adequate transfer of both lateral and torsional restraint from the sheeting to the purlin. If adequate lateral restraint and some degree of torsional restraint is applied, both Z-sections and channels will undergo vertical deflection and twisting, including section distortion, as shown in Fig. 1(a) for a simple Z-section and in Fig. 1(b) for a simple channel. Peköz and Soroushian (1982) proposed that the vertical bending stage be analysed using simple flexure theory, whilst the torsion stage be analysed by modelling the unconnected purlin flange, lip, and a section of the web as a beam-column on an elastic foundation. The stiffness of the foundation is idealised as a linear extensional spring of stiffness k, located at the level of the unconnected purlin flange as shown in Fig. 1(c).

When a uniformly distributed wind uplift or gravity load, q, is applied parallel with the purlin web, a uniformly distributed lateral load, w, is induced in the unconnected purlin flange. Peköz and Soroushian calculated the lateral load induced in the unconnected flange of a simply-supported Z-section purlin under wind uplift loading as being equal to

$$w = q(\frac{Qb}{2\,I_x}) \tag{1}$$

where Q is the first moment of area of the beam-column section about the purlin centroidal x-axis perpendicular to the web, b is the total width of the unconnected purlin flange, and I_x is the second moment of area of the full or effective deflected purlin section about the centroidal x-axis perpendicular to the undeflected position of the web.

As a result of lateral deflection and twist, the second moment of area, I_x, is reduced according to the equation (Peköz and Soroushian, 1982)

$$I_x = I_{x0}[1 - (\frac{\delta}{H})^2] \tag{2}$$

where

I_{x0} = second moment of area of the full or effective *un*deflected purlin section about the centroidal x-axis perpendicular to the web
H = purlin web depth
δ = lateral deflection of the unconnected purlin flange

Peköz and Soroushian suggested that Q could be simplified by ignoring the contributions of the purlin web and lip to the beam-column section, whereas Thomasson (1988) included both the lip and a section of the web of depth x in his calculations. Rousch, Rasmussen and Hancock (1993) demonstrated that Eq. 1 is valid for both simply-supported *and* continuous simple Z-section *and* simple channel purlins under wind uplift loading when substantial torsional restraint is provided by the sheeting. The calculation of the beam-column moment, Q, should include the contribution of both the lip and a section of the web of depth x. For Australian made Z-sections and channels, x should be taken as being equal to 35 percent of the total web depth. The second moment of area, I_x, should be that of the *full* purlin section.

Fig. 2(a) shows the beam-column section for a typical simply-supported purlin-sheeting system without bridging (bracing), including the axial compressive force, p, induced in the unconnected purlin flange by the in-plane bending, the induced uniformly distributed lateral load, w, given by Eq. 1, and the torsional restraint provided by the sheeting to the purlin, represented by a lateral restraint of stiffness k. Fig. 2(b) shows the same beam-column section with one row of bridging at the midspan, which effectively prevents lateral displacement of the unconnected purlin flange at that point. The bridging restraint is represented by a single spring of stiffness k_B.

2.2 Failure Criteria

The stress distribution in the unconnected (compression) purlin flange of a screw-fastened channel or Z-section purlin under wind uplift loading can be calculated from the in-plane bending stresses determined from a linear, in-plane analysis, and the out-of-plane bending stresses determined from the non-linear, out-of-plane analysis developed by Rousch and Hancock (1994a, 1994b).

Analytical Stresses

The in-plane bending stress, σ_i, induced in the compression flange of a channel or Z-section purlin is given by the equation

$$\sigma_i = \frac{M_x}{Z_x} \tag{3}$$

where

M_x = in-plane bending moment
Z_x = elastic section modulus of the full deflected purlin section for the extreme compression fibre for bending of the whole section about the x-axis perpendicular to the web

The in-plane bending stress, σ_i, is assumed constant across the width of the unconnected (compression) purlin flange.

The out-of-plane bending stress, σ_o, induced in the compression flange of a channel or Z-section purlin is given by the equation

$$\sigma_o = \frac{M_{ybc}}{Z_{ybc}} \tag{4}$$

where

M_{ybc} = out-of-plane bending moment applied to the beam-column section, comprised of the unconnected purlin flange, lip, and 35 percent of the web
Z_{ybc} = elastic section modulus of the beam-column section for bending about the centroidal y-axis of the beam-column section parallel with the web

The out-of-plane bending stress, σ_o, can be calculated at any point along the unconnected purlin flange.

The total stress, σ_f, at any point along the unconnected purlin flange is therefore given by the equation

$$\sigma_f = \sigma_i + \sigma_o = \frac{M_x}{Z_x} + \frac{M_{ybc}}{Z_{ybc}} \tag{5}$$

Distortional Buckling Failure Stress

A design method for the distortional buckling of flexural members has been presented by Hancock, Rogers and Schuster (1996). Distortional buckling of flexural members such as channel and Z-section purlins usually involves the rotation of the compression flange and lip about the flange-web junction, as shown in Fig. 3(a). The web undergoes flexure at the same half-wavelength as the flange buckle, and the compression flange may translate in a direction normal to the web. The flexure of the web involves double curvature transverse bending. The calculation rules applied by Hancock in the design for distortional buckling of channel and Z-section purlins which are prevented from twisting so that there is uniform compression across the flanges as shown in Fig. 3(b), are given in Eqs 6(a) and 6(b). The alternative equations for distortional buckling, which are based on a strength design curve that has been upgraded slightly from the original proposal, are given in Eqs 7(a) and 7(b).

The distortional buckling failure stress, σ_c, in the compression flange of a channel or Z-section purlin can be calculated from the elastic distortional buckling stress, σ_{od}, and the yield stress, f_y, as follows.

For $\sigma_{od} > 0.5 f_y$:

$$\sigma_c = f_y[1 - \frac{f_y}{4\,\sigma_{od}}] \tag{6a}$$

and for $\sigma_{od} \leq 0.5 f_y$:

$$\sigma_c = f_y[0.055(\sqrt{\frac{f_y}{\sigma_{od}}} - 3.6)^2 + 0.237] \tag{6b}$$

Alternatively, for $\sigma_{od} > 2.2 f_y$:

$$\sigma_c = f_y \tag{7a}$$

and for $\sigma_{od} \leq 2.2 f_y$:

$$\sigma_c = f_y \sqrt{\frac{\sigma_{od}}{f_y}}(1 - 0.22\sqrt{\frac{\sigma_{od}}{f_y}}) \tag{7b}$$

The elastic distortional buckling stress, σ_{od}, can be calculated from the equations provided in Appendix A of Hancock, Rogers and Schuster, in Appendix D of the amended draft Australian/New Zealand *Cold-Formed Steel Structures Standard* (Standards Australia/Standards New Zealand, 1996), or by a rational analysis (Papangelis and Hancock, 1995). These equations include the full section properties of the compression flange and lip.

Local (Flange-Web) Buckling Failure Stress

The local buckling failure stress, σ_{bw}, at the purlin flange-web junction can be determined from the equations in the Australian *Cold-Formed Steel Structures Code*, AS 1538 (Standards Association of Australia, 1988), with the factor of safety removed:

$$\sigma_{bw} = [1.21 - 0.00013(\frac{d_1}{t})\sqrt{f_y}]\, f_y \tag{8}$$

where

d_1 = clear distance between the flanges
t = nominal steel thickness exclusive of coatings
f_y = yield stress of the steel

Comparison of Stresses

The distortional buckling failure stress, σ_c, calculated in the compression flange of a channel or Z-section purlin using Eqs 6 or 7, can be compared with the analytical stress, σ_{fl}, calculated at the purlin flange-lip junction using Eq. 5. The flange of the section usually has a stress gradient across it when failure occurs, as shown in Fig. 3(c). Equations 6 and 7 are based on uniform stress in the flange, but it is assumed that these equations still applicable. The local buckling

failure stress, σ_{bw}, calculated at the purlin flange-web junction using Eq. 8, can be compared with the analytical stress, σ_{fw}, calculated at the flange-web junction using Eq. 5.

The distortional buckling failure stress, σ_c, and the local buckling failure stress, σ_{bw}, can therefore be used in the non-linear analysis to predict the limit states of screw-fastened purlins under wind uplift loading. In the analysis, the applied uniformly distributed wind uplift load, q, is increased from zero until either $\sigma_{fl} = \sigma_c$ or $\sigma_{fw} = \sigma_{bw}$ occurs at some point along the purlin span. If $\sigma_{fl} = \sigma_c$, a distortional buckling failure mode is predicted by the analysis. If $\sigma_{fw} = \sigma_{bw}$, a local (flange-web) buckling failure mode is predicted. The load at which this occurs is the predicted purlin failure load, q_f.

3 VACUUM RIG TEST RESULTS

3.1 General

Simulated wind uplift tests on roof and wall systems composed of simply-supported and continuous cold-formed simple channel and simple Z-section purlins screw-fastened to sheeting have been performed in the vacuum test rig at the Centre for Advanced Structural Engineering (1989, 1990, 1994) within the University of Sydney. These included the Series 1 - 3 tests, the results of which have been published in Hancock *et al* (1990, 1993), and the Series 7 tests, published in Rousch and Hancock (1995a, 1995b).

The non-linear analysis developed by Rousch and Hancock (1994a, 1994b) and outlined in Section 2 of this paper has been used to predict the failure loads and failure modes of the Series 1 - 3 and Series 7 vacuum rig tests. The non-linear analysis incorporates the torsional restraint, k, provided by the sheeting to the attached purlin, and the bridging restraint, k_B, as discussed in Section 2. The value of the torsional restraint, k, has been determined for the purlins in each of the Series 1 - 3 and Series 7 vacuum rig tests from purlin-sheeting connection tests carried out at the University of Sydney by Rousch and Hancock (1996). The test procedure employed was similar to the purlin-sheeting connection test method described in the AISI *Test Procedures* (1986). Rousch and Hancock reported that torsional restraint is dependent on the position of the screw-fastener across the purlin flange. For this reason, the purlins in the Series 7 vacuum rig tests were carefully screw-fastened at the mid-flanges (Rousch and Hancock, 1995a, 1995b). The same care in aligning the screws was not administered to the purlins in the Series 1 - 3 tests conducted earlier, however these have also been assumed to be screw-fastened at the mid-flanges.

The value of the bridging restraint, k_B, is dependent on whether the rotations at the purlin end supports (cleats) are assumed to be fixed or free in the non-linear analysis for the bending of the beam-column section about an axis parallel with the purlin web. The fixed end rotation case assumes that the cleats completely prevent minor axis bending of the purlin, whilst the free end rotation case assumes that the cleats provide no restraint to minor axis bending. The restraint provided (Rousch and Hancock, 1995a) by one row of bridging in each purlin span is equal to 78 N/mm when the end rotations at the cleats are assumed fixed, and 88 N/mm when the end rotations are assumed free. The restraint provided by two rows of bridging in each purlin span is equal to 101 N/mm when the end rotations are assumed fixed, and 88 N/mm when the end rotations are assumed free.

The data for each of the Series 1 - 3 and Series 7 vacuum rig tests is included in Table 1. This data includes the purlin type, the number of spans, the number of rows of bridging in each span,

and the measured torsional restraint, k, provided to each purlin by the attached sheeting.

3.2 Comparison of Tests with Non-Linear Analysis

The experimental failure load, q_{Exp}, of each of the Series 1-3 and Series 7 vacuum rig tests is given in Table 2. As discussed in Section 2.2, the distortional buckling failure stress, σ_c, and the flange-web buckling failure stress, σ_{bw}, are used in the non-linear analysis to predict the failure load and failure mode of the purlins in each vacuum rig test. The values of σ_c and σ_{bw}, calculated for the purlins in each vacuum rig test using Eqs 7 and 8 respectively, and the failure loads, $q_{f_{Fixed}}$ and $q_{f_{Free}}$, predicted by the anaylsis when the rotations at the purlin end supports are assumed fixed and free respectively, are given in Table 2. The ratios, $q_{Exp}/q_{f_{Fixed}}$ and $q_{Exp}/q_{f_{Free}}$, of the experimental failure load to the predicted failure loads are also given for each test in Table 2.

The ratio of the analytical stress, σ_{fl}, calculated at the purlin flange-lip junction at failure, to the distortional buckling failure stress, σ_c, and the ratio of the analytical stress, σ_{fw}, calculated at the purlin flange-web junction at failure, to the local buckling failure stress, σ_{bw}, are given in Table 3 for both cases of fixed and free rotations at the purlin end supports. A ratio of σ_{fl}/σ_c equal to 1.0 indicates a predicted failure mode of distortional buckling, whilst a ratio of σ_{fw}/σ_{bw} equal to 1.0 indicates a predicted failure mode of flange-web buckling. From the ratios in Table 3, it can be seen that, in some tests, the purlins are predicted to fail by either distortional buckling or by flange-web buckling, as both ratios are close to unity. This is particularly the case for the purlins in the unbridged tests.

The predicted failure modes and their locations along each purlin span are compared with the actual vacuum rig test failures in Fig. 4 for Series 1, Fig. 5 for Series 2, Fig. 6 for Series 3 and Fig. 7 for Series 7. For the cases where both distortional and flange-web buckling failure are a possibility, the failure (mode and location) which best matches the actual test failure has been chosen. These failures are indicated in Table 3 in *italics*. In all but four cases (Series 1 Test 4(A), Series 2 Tests 2 and 3, and Series 3 Test 3), the failure predicted by the non-linear analysis when the end rotations are assumed fixed is the same as that predicted when the end rotations are assumed free. The failure predicted for Series 1 Test 4(A) best matches the actual test failure when the end rotations are free, whilst the failures predicted for Series 2 Tests 2 and 3 and Series 3 Test 3 best match the actual test failures when the end rotations are fixed.

From Figs 4-7 it can be seen that there is very good correlation between the predicted failures and the actual failures for all tests except Series 1 Test 6. The purlins in this test failed by distortional buckling at the end of a lap in the interior span, not, as predicted by the analysis, by distortional buckling at the bridging. Failure at the end of a lap indicates that perhaps larger purlin sections, Z20019 sections for example, were used in one or both of the end spans instead of Z20015 sections as specified. (It is common practice in industry to use a larger section if the section specified is not available.) The relatively high ratios of $q_{Exp}/q_{f_{Fixed}}$ and $q_{Exp}/q_{f_{Free}}$ for Series 1 Test 6, equal to 1.395 and 1.479 respectively, support this theory.

The mean ratios of $q_{Exp}/q_{f_{Fixed}}$ and $q_{Exp}/q_{f_{Free}}$ for the tests with no bridging, one row of bridging and two rows of bridging have been tabulated, along with the corresponding standard deviations, in Table 4. Series 1 Test 6 has been excluded from these calculations. The values in Table 4 indicate that the non-linear analysis predicts failure loads closer to those determined experimentally when the end rotations are assumed to be fixed than when they are assumed to be free.

4 DESIGN CRITERIA

4.1 Reliability Analysis

The reliability or safety index, β, is a relative measure of the reliability or safety of a structure or structural element. When two designs are compared, the one with the larger β is the more reliable. The reliability index accounts for the uncertainties and variabilities inherent in the design parameters, such as the material properties, geometry, and applied load.

To calculate the reliability index, a First Order Second Moment (FOSM) method, described by Ellingwood *et al* (1980), can be used. This method is outlined in the AISI Commentary (1991b). Because of the uncertainties and variabilities in the applied load, Q, and resistance, R, the exact probability distributions of Q and R (both assumed to have lognormal distributions) are not known. However, the mean applied load, Q_m, and mean resistance, R_m, and the corresponding variances V_Q and V_R, can be used to calculate the reliability index, β:

$$\beta = \frac{ln(R_m/Q_m)}{\sqrt{V_R^2 + V_Q^2}} \tag{9}$$

The mean resistance, R_m, is given by the equation

$$R_m = R_n \cdot (P_m \cdot M_m \cdot F_m) \tag{10}$$

where R_n is the nominal resistance, and

P_m	=	mean ratio of the experimentally determined failure load to the predicted failure load for the actual material and cross-sectional properties of the test specimens
M_m	=	mean ratio of the actual yield stress to the minimum specified (nominal) yield stress
F_m	=	mean ratio of the actual specimen thickness to the nominal thickness

The variance V_R is given by the equation

$$V_R = \sqrt{V_P^2 + V_M^2 + V_F^2} \tag{11}$$

where V_P, V_M and V_F are the variances of P, M and F respectively.

The nominal resistance, R_n, for a screw-fastened purlin under wind uplift loading must satisfy the equation

$$Q \leq \phi \cdot R_n \tag{12}$$

where ϕ is the resistance (or capacity) factor, and

$$Q = W_u - 0.8\,G \tag{13}$$

W_u and G are the applied wind uplift and dead loads respectively. The load combination $W_u - 0.8 \cdot G$ is given in the Australian loading code, AS 1170.1 (Standards Association of Australia, 1989a).

As mentioned earlier, the exact probability distributions of Q, and hence of W_u and G, are not known. However, the mean load, Q_m, can be expressed as

$$Q_m = W_{u_m} - G_m \tag{14}$$

where W_{u_m} and G_m are the mean wind uplift and dead loads respectively. The corresponding variance, V_Q, is given by the equation (AISI Commentary, 1991b)

$$V_Q = \frac{\sqrt{(W_{u_m} V_W)^2 + (G_m V_G)^2}}{W_{u_m} - G_m} \tag{15}$$

where V_W and V_G are the variances of W_u and G respectively. Ellingwood *et al* analysed load statistics to show that $G_m = 1.05G$ and $V_G = 0.1$. The value of 1.05 indicates that dead loads are, on average, underestimated. Holmes (1995) derived the parameters $W_{u_m} = 0.42W_u$ and $V_W = 0.37$ by application of the Australian wind loading code, AS 1170.2 (1989b).

From Eqs 12-14, and by assuming that $G_m = 1.05G$, $W_{u_m} = 0.42W_u$, and $G/W_u = 0.1$,

$$Q_m \leq 0.342 \cdot \phi \cdot R_n \tag{16}$$

By substituting $V_G = 0.1$ and $V_W = 0.37$ into Eq. 15, $V_Q = 0.494$.

Substitution of Eqs 10, 11, 16 and $V_Q = 0.494$ into Eq. 9 gives

$$\beta = \frac{ln((P_m \cdot M_m \cdot F_m)/0.342 \cdot \phi)}{\sqrt{V_P^2 + V_M^2 + V_F^2 + 0.494^2}} \tag{17}$$

The resistance factor, ϕ, can be calculated for a fixed target value of the reliabilty index, $\beta = 2.5$ (AISI Commentary, 1991b).

From the experimental and predicted failure loads given in Table 2, the resistance factors of both the bridged and unbridged purlins have been calculated using Eq. 17 with $\beta = 2.5$. These resistance factors, together with the parameters P_m, V_m, F_m and their corresponding variances, V_P, V_M and V_F, are given in Table 5. The resistance factors 0.913 and 0.9, calculated for the unbridged purlins when the end rotations in the non-linear analysis are assumed fixed and free respectively, imply that the non-linear analysis is unconservative when estimating the failure loads of unbridged purlins, and so the predicted failure loads may need to be factored down. The resistance factors 0.992 and 1.131, calculated for the bridged purlins when the end rotations in the non-linear analysis are assumed fixed and free respectively, imply that the analysis is very accurate when estimating the failure loads of bridged purlins when fixed end rotations are assumed, but conservative when free end rotations are assumed.

4.2 Reduction Factors

Clause 3.3.3.3 of the amended draft *Australian/New Zealand Cold-Formed Steel Structures Standard* (Standards Australia/Standards New Zealand, 1996) states that the nominal member moment capacity, M_b, of a channel or Z-section purlin loaded in a plane parallel with the web, and with the tension flange attached to sheeting and the compression flange laterally unbraced, is given by the equation

$$M_b = R \cdot Z_{xeff} \cdot f_y \tag{18}$$

where

f_y = yield stress
R = reduction factor
Z_{xeff} = elastic section modulus of the effective deflected purlin section for the extreme compression fibre at f_y for bending of the whole section about the x-axis perpendicular to the web

The reduction factors, or R-factors, in the draft standard were calibrated by Johnston and Hancock (1994) from the Series 1-3 vacuum rig tests (Centre for Advanced Structural Engineering, 1989, 1990).

From the failure loads, $q_{f_{Fixed}}$ and $q_{f_{Free}}$, predicted by the non-linear analysis (assuming fixed end rotations and free end rotations respectively) for the purlins in each of the Series 1-3 and Series 7 vacuum rig tests and given in Table 2, nominal member moment capacities, $M_{b_{Fixed}}$ and $M_{b_{Free}}$, can be calculated. Hence, from Eq. 18, corresponding R-factors, R_{Fixed} and R_{Free}, can be determined. The values of f_y, Z_{xeff}, $M_{b_{Fixed}}$ and R_{Fixed}, and $M_{b_{Free}}$ and R_{Free} are given for the purlins in each vacuum rig test in Table 6.

From the R-factors, R_{Fixed} and R_{Free}, determined for each purlin test, average R-factors have been calculated for the simply-supported and three-span continuous tests with no bridging, one row of bridging and two rows of bridging, and for the two-span continuous tests with no bridging, one row of bridging and two rows of bridging. Series 1 Test 6 has been excluded from these calculations. The average R-factors are compared with the R-factors given in the draft Australian/New Zealand standard in Table 7.

Generally, the R-factors calculated from the analysis assuming fixed end rotations, R_{Fixed}, are closer to the values in the draft standard than those calculated assuming free end rotations, R_{Free}. For the simply-supported and three-span continuous tests, R_{Fixed} is close to the value in the draft standard for the no bridging case, but conservative for one and two rows of bridging. For the two-span continuous tests, R_{Fixed} is close to the value in the draft standard for the one row of bridging case, but unconservative for the no bridging and two rows of bridging cases.

Part of the discrepancy between the average R-factors, R_{Fixed} and R_{Free}, determined from the predicted failure loads, and the R-factors in the draft standard, can be explained. Firstly, Johnston and Hancock calculated the R-factor for each of the Series 1 - 3 vacuum rig tests using a nominal yield stress, f_y, of 450 MPa, whereas R_{Fixed} and R_{Free} were calculated using the actual purlin yield stress, given in Table 6. Secondly, the R-factors in the draft standard were calculated from the average R-factors *minus one standard deviation.* There is also a possibility that the value of $R = 1.0$ given in the draft standard for the simply-supported and three-span continuous cases with two rows of bridging may need to be adjusted down to 0.95 if the Series

1 Test 6 results are removed from the data as discussed earlier.

5 CONCLUSION

A non-linear, out-of-plane elastic analysis has been developed at the University of Sydney by Rousch and Hancock to predict the failure loads, failure modes and R-factors of simply-supported and continuous cold-formed simple channel and simple Z-section purlins screw-fastened to sheeting, and subject to wind uplift loading. The distortional and local (flange-web) buckling failure stresses were used in the analysis to predict the purlin limit states. The rotations at the purlin end supports (cleats) for the bending of the beam-column section about an axis parallel with the purlin web were assumed, in the first instance, to be fixed, and in the second, to be free. The predicted failures have been compared with those obtained experimentally in the Series 1 - 3 and Series 7 vacuum rig tests performed at the Centre for Advanced Structural Engineering within the University of Sydney. The predicted R-factors have been compared with those in the amended draft Australian/New Zealand *Cold-Formed Steel Structures Standard.*

Several observations can be made as a result:

1. The failure modes predicted by the non-linear analysis, assuming either fixed or free end rotations at the cleats, compare closely with those obtained experimentally in the Series 1 - 3 and Series 7 vacuum rig tests. The failure loads predicted assuming fixed end rotations are, on average, 7 percent higher than those predicted assuming free end rotations, and are closer to the experimental failure loads.

2. Calculation of resistance factors showed that the non-linear analysis assuming either fixed or free end rotations at the cleats is unconservative when estimating the failure loads of unbridged purlins, and so the predicted failure loads may need to be factored down. When estimating the failure loads of bridged purlins, the analysis is very accurate when assuming fixed end rotations, but conservative when assuming free end rotations.

3. The R-factors predicted by the analysis assuming fixed end rotations compare more closely with the R-factors in the draft standard than do those predicted assuming free end rotations. This is particularly the case for purlins with one row of bridging.

   The value of $R = 1.0$ given in the draft standard for the simply-supported and three-span continuous purlins with two rows of bridging appears unconservative, and may need to be adjusted down to 0.95.

From the above observations it can be concluded that the non-linear analysis developed by Rousch and Hancock can be successfully used to determine the failure loads, failure modes and R-factors of roof and wall systems composed of simply-supported and continuous screw-fastened simple channel and simple Z-section purlins, and subject to wind uplift loading. The rotations at the cleats should be fixed in the analysis to prevent minor axis bending of the purlin.

ACKNOWLEDGEMENTS

This paper forms part of a programme of research into the behaviour and design of thin-walled metal structures being undertaken in the School of Civil and Mining Engineering within the University of Sydney. The Series 1, 2, 3 and 7 tests were performed in the Vacuum Type Purlin Test Rig, funded by the Metal Building Products Manufacturers Association, in the J.W. Roderick Laboratory for Materials and Structures. The first author is supported by a joint Metal Building Products Manufacturers Association and Civil and Mining Engineering Foundation Scholarship. The Series 7 tests were partially funded by an ARC Collaborative Research Grant with BHP Building Products.

APPENDIX A. REFERENCES

American Iron and Steel Institute (1986), *Test Procedures* for use with the August 19, 1986 Edition of the *Specification for the Design of Cold-Formed Steel Structural Members*, Washington D.C., U.S.A.

American Iron and Steel Institute (1991a), *Load and Resistance Factor Design Specification for Cold-Formed Steel Structural Members*, Washington D.C., U.S.A.

American Iron and Steel Institute (1991b), *Commentary on the Load and Resistance Factor Design Specification for Cold-Formed Steel Structural Members*, Washington D.C., U.S.A.

Centre for Advanced Structural Engineering (1989, 1990), "Vacuum Test Rig Common Purlin Test Program Series 1, 2 & 3", Investigation Reports S754, S761, S768, School of Civil and Mining Engineering, The University of Sydney, Australia.

Centre for Advanced Structural Engineering (1994), "Vacuum Test Rig Common Purlin Test Programme Series 7 - Simply Supported Z-Sections and Channels with Full Instrumentation", Investigation Report S989, School of Civil and Mining Engineering, The University of Sydney, Australia.

Ellingwood, B., Galambos, T.V., MacGregor, J.G. and Cornell, C.A. (1980), "Development of a Probability Based Load Criterion for American National Standard A58: Building Code Requirements for Minimum Design Loads in Buildings and Other Structures", NBS Special Publication No. 577, National Bureau of Standards, Washington DC, U.S.A.

Hancock, G.J., Celeban, M., Healy, C., Georgiou, P.N. and Ings, N.L. (1990), "Tests of Purlins with Screw-Fastened Sheeting under Wind Uplift", *Tenth International Specialty Conference on Cold-Formed Steel Structures*, University of Missouri-Rolla, St Louis, Missouri, U.S.A.

Hancock, G., Celeban, M. and Healy, C. (1993), "Behaviour of Purlins with Screw Fastened Sheeting under Wind Uplift and Downwards Loading", *Australian Civil Engineering Transactions*, Vol. CE35 No. 3, pp 221-233.

Hancock, G.J., Rogers, C.A. and Schuster, R.M. (1996), "Comparison of the Distortional Buckling Method for Flexural Members with Tests", accepted for publication, *Thirteenth International Specialty Conference on Cold-Formed Steel Structures*, University of Missouri-Rolla, St Louis, Missouri, U.S.A.

Holmes, J.D. (1985), "Wind Loads and Limit States Design", *Civil Engineering Transactions*, Vol. CE27 No. 1, pp 21-26.

Johnston, N. and Hancock, G. (1994), "Calibration of the AISI R-factor design approach for purlins using Australian test data", *Engineering Structures*, Vol. 16 No. 5, pp 342-347.

Papangelis, J.P. and Hancock, G.J. (1995), "Computer Analysis of Thin-Walled Structural Members", *Computers & Structures*, Vol. 56 No. 1, pp 157-176.

Peköz, T. and Soroushian, P. (1982), "Behaviour of C- and Z- Purlins Under Wind Uplift", *Sixth International Specialty Conference on Cold-Formed Steel Structures*, pp 409-429, University of Missouri-Rolla, St Louis, Missouri, U.S.A.

Rousch, C.J. and Hancock, G.J. (1994a), "A Non-Linear Analysis Model for Simply-Supported and Continuous Purlins", Research Report R688, School of Civil and Mining Engineering, The University of Sydney, Australia.

Rousch, C.J. and Hancock, G.J. (1994b), "Comparison of a Non-Linear Purlin Model with Tests", *Twelfth International Specialty Conference on Cold-Formed Steel Structures*, pp 121-149, University of Missouri-Rolla, St Louis, Missouri, U.S.A.

Rousch, C.J. and Hancock, G.J. (1995a), "Tests of Channel and Z-Section Purlins Undergoing Non-Linear Twisting", Research Report R708, School of Civil and Mining Engineering, The University of Sydney, Australia.

Rousch, C.J. and Hancock, G.J. (1995b), "Comparison of Tests of Bridged and Unbridged Purlins with a Non-Linear Analysis Model", *Fourth Pacific Structural Steel Conference*, Singapore.

Rousch, C.J. and Hancock, G.J. (1996), "Purlin-Sheeting Connection Tests", Research Report R724, School of Civil and Mining Engineering, The University of Sydney, Australia.

Rousch, C.J., Rasmussen, K.J.R. and Hancock, G.J. (1993), "Bending Strengths of Cold-Formed Channel and Z Sections Restrained by Sheeting", *International Workshop on Cold-Formed Steel Structures*, Sydney, Australia.

Standards Association of Australia (1988), AS 1538 *Cold-Formed Steel Structures Code*, North Sydney, Australia.

Standards Association of Australia (1989a), AS 1170.1 *SAA Loading Code, Part 1: Dead and live loads and load combinations*, North Sydney, Australia.

Standards Association of Australia, (1989b), AS 1170.2 *SAA Loading Code, Part 1: Wind loads*, North Sydney, Australia.

Standards Australia/Standards New Zealand (1996), Draft *Cold-Formed Steel Structures Standard* (BD/82/96-12), North Sydney, Australia.

Thomasson, P.O. (1988), "On the Behaviour of Cold-Formed Steel Purlins - Particularly with Respect to Cross Sectional Distortion", *Baehre-Festschrift*, pp 281-292, Karlsruhe, Germany.

APPENDIX B. NOTATION

b	width of unconnected purlin flange
d_1	clear distance between flanges
f_y	yield stress
F_m	mean ratio of actual specimen thickness to nominal thickness
G	dead load
G_m	mean dead load
H	purlin web depth
I_x	second moment of area of full deflected purlin section
I_{x0}	second moment of area of full undeflected purlin section
k	torsional restraint
k_B	bridging restraint
M_b	nominal member moment capacity
M_m	mean ratio of actual yield stress to nominal yield stress
M_x	in-plane bending moment
M_{ybc}	out-of-plane bending moment
p	induced distributed axial compressive force
P_m	mean ratio of experimentally determined failure load to predicted failure load
q	applied uniformly distributed wind uplift or gravity load
q_f	predicted failure load
q_{Exp}	experimental failure load
Q	first moment of area of beam-column section *or* applied load
Q_m	mean applied load
R	resistance *or* reduction factor
R_m	mean resistance
R_n	nominal resistance
t	purlin thickness
V_F, V_M, V_P, V_Q, V_R	variances of F, M, P, Q and R respectively
w	induced uniformly distributed lateral load
W_u	wind uplift load
W_{u_m}	mean wind uplift load
x	depth of purlin web included in beam-column section
Z_x	elastic section modulus of full deflected purlin section
Z_{xeff}	elastic section modulus of effective deflected purlin section
Z_{ybc}	elastic section modulus of beam-column section
β	reliability index
δ	lateral deflection of unconnected purlin flange
σ_{bw}	flange-web buckling failure stress
σ_c	distortional buckling failure stress
σ_f	total stress
σ_{fl}	stress at purlin flange-lip junction
σ_{fw}	stress at purlin flange-web junction
σ_i	in-plane bending stress
σ_o	out-of-plane bending stress
σ_{od}	elastic distortional buckling stress
ϕ	resistance factor

Test	Purlin Type	No. Spans	Bridging	k (N/mm^2)
S1T1	Z15019	3-span continuous	0-0-0	0.058
S1T2	Z15019	3-span continuous	1-1-1	0.058
S1T3	Z15019	3-span continuous	2-1-2	0.058
S1T4(A)	Z20015	3-span continuous	0-0-0	0.014
S1T5	Z20015	3-span continuous	1-1-1	0.014
S1T6	Z20015	3-span continuous	2-1-2	0.014
S1T7	Z20019	3-span continuous	0-0-0	0.026
S1T8	Z20019	3-span continuous	1-1-1	0.026
S1T9	Z20019	3-span continuous	2-1-2	0.026
S2T1	Z30025	2-span continuous	0-0	0.016
S2T2	Z30025	2-span continuous	1-1	0.016
S2T3	Z30025	2-span continuous	2-2	0.016
S3T1(R)	Z20024	simply-supported	0	0.041
S3T2	Z20024	simply-supported	1	0.041
S3T3	Z20024	simply-supported	2	0.041
S3T4	C20024	simply-supported	0	0.028
S3T5	C20024	simply-supported	1	0.028
S3T6	C20024	simply-supported	2	0.028
S7T1	Z20015	simply-supported	0	0.023
S7T2	C20015	simply-supported	0	0.018
S7T3	C20015	simply-supported	1	0.018
S7T5	C20015	simply-supported	2	0.018

Table 1: Series 1 - 3 and Series 7 Vacuum Rig Test Data

Test	q_{Exp} (N/mm)	σ_c (MPa)	σ_{bw} (MPa)	Fixed End Rotations		Free End Rotations	
				q_{Fixed} (N/mm)	q_{Exp}/q_{Fixed}	q_{Free} (N/mm)	q_{Exp}/q_{Free}
S1T1	2.31	374	488	3.003	0.769	2.988	0.773
S1T2	2.63	374	488	2.419	1.087	2.234	1.177
S1T3	2.98	391	488	2.563	1.163	2.438	1.222
S1T4(A)	2.58	318	436	2.369	1.089	2.422	1.065
S1T5	2.94	318	436	2.400	1.225	2.153	1.366
S1T6	3.87	318	436	2.775	1.395	2.616	1.479
S1T7	3.51	352	461	3.594	0.977	3.566	0.984
S1T8	4.28	352	461	3.600	1.189	3.188	1.343
S1T9	4.55	352	461	3.988	1.141	3.800	1.197
S2T1	4.33	352	431	4.456	0.972	4.244	1.020
S2T2	4.93	341	431	5.256	0.938	3.988	1.236
S2T3	5.77	342	427	6.275	0.920	5.763	1.001
S3T1(R)	3.28	385	517	3.644	0.900	3.806	0.862
S3T2	3.69	385	517	4.113	0.897	3.231	1.142
S3T3	4.76	385	517	4.075	1.168	4.025	1.183
S3T4	3.63	400	507	3.122	1.163	3.231	1.123
S3T5	3.63	400	507	4.338	0.837	3.094	1.173
S3T6	4.71	400	507	3.906	1.206	3.994	1.179
S7T1	1.85	331	439	1.922	0.963	2.006	0.922
S7T2	1.70	320	454	1.844	0.922	1.919	0.886
S7T3	1.77	311	431	1.675	1.057	1.434	1.234
S7T5	1.95	311	430	1.878	1.038	1.866	1.045

Table 2: Comparision of Failure Loads

Test	Fixed End Rotations			Free End Rotations		
	σ_{fl}/σ_c	σ_{fw}/σ_{bw}	Buckling Mode	σ_{fl}/σ_c	σ_{fw}/σ_{bw}	Buckling Mode
S1T1	0.86	1.00	*Flange-Web*	1.00	0.96	*F-W*/Dist.
S1T2	1.00	0.66	*Distortional*	1.00	0.62	*Distortional*
S1T3	1.00	0.75	*Distortional*	1.00	0.67	*Distortional*
S1T4(A)	1.00	0.87	Distortional	0.96	1.00	*F-W*/Dist.
S1T5	1.00	0.65	*Distortional*	1.00	0.56	*Distortional*
S1T6	1.00	0.74	Distortional	1.00	0.65	Distortional
S1T7	1.00	0.96	*F-W*/Dist.	0.94	1.00	*F-W*/Dist.
S1T8	1.00	0.74	*Distortional*	1.00	0.57	*Distortional*
S1T9	1.00	0.81	*Distortional*	1.00	0.71	*Distortional*
S2T1	1.00	0.99	*F-W*/Dist.	0.78	1.00	*Flange-Web*
S2T2	1.00	0.94	*F-W*/Dist.	1.00	0.72	Distortional
S2T3	1.00	0.97	*F-W*/Dist.	1.00	0.92	F-W/Dist.
S3T1(R)	0.93	1.00	*F-W*/Dist.	0.86	1.00	*Flange-Web*
S3T2	1.00	0.87	*Distortional*	1.00	0.63	*Distortional*
S3T3	1.00	0.95	*F-W*/Dist.	1.00	0.86	Distortional
S3T4	0.92	1.00	*F-W*/Dist.	0.80	1.00	*Flange-Web*
S3T5	0.98	1.00	F-W/*Dist.*	1.00	0.63	*Distortional*
S3T6	0.98	1.00	F-W/*Dist.*	1.00	0.94	F-W/*Dist.*
S7T1	0.93	1.00	*F-W*/Dist.	0.89	1.00	*Flange-Web*
S7T2	0.99	1.00	*F-W*/Dist.	0.87	1.00	*Flange-Web*
S7T3	1.00	0.67	*Distortional*	1.00	0.55	*Distortional*
S7T5	1.00	0.85	*Distortional*	1.00	0.80	*Distortional*

Table 3: Predicted Failure Modes

	Fixed End Rotations		Free End Rotations	
	Mean q_{Exp}/q_{Fixed}	Standard Deviation	Mean q_{Exp}/q_{Free}	Standard Deviation
No Bridging	0.969	0.119	0.954	0.115
1 Row Bridging	1.033	0.148	1.239	0.086
2 Rows Bridging *	1.106	0.107	1.138	0.092

Table 4: Calculated Means - Series 1 - 3 and Series 7 (*excludes Series 1 Test 6)

$\beta = 2.5$	M_m	V_M	F_m	V_F	P_m	V_P	ϕ
Unbridged Purlins Fixed End Rotations	1.142	0.044	1.012	0.007	0.969	0.123	0.913
Unbridged Purlins Free End Rotations	1.142	0.044	1.012	0.007	0.954	0.121	0.900
Bridged Purlins Fixed End Rotations	1.123	0.034	1.014	0.006	1.067	0.123	0.992
Bridged Purlins Free End Rotations	1.123	0.034	1.014	0.006	1.192	0.084	1.131

Table 5: Resistance Factors - Series 1 - 3 and Series 7

Test	f_y (MPa)	Z_{xeff} (mm^3)	$M_{b_{Fixed}}$ (kNm)	R_{Fixed}	$M_{b_{Free}}$ (kNm)	R_{Free}
S1T1	487	2.447E+4	11.38	0.955	11.32	0.950
S1T2	487	2.447E+4	9.17	0.769	8.47	0.710
S1T3	487	2.389E+4	9.71	0.835	9.24	0.794
S1T4(A)	520	2.612E+4	8.98	0.661	9.18	0.676
S1T5	520	2.612E+4	9.10	0.670	8.16	0.601
S1T6	520	2.612E+4	10.52	0.774	9.92	0.730
S1T7	495	3.800E+4	13.62	0.724	13.52	0.719
S1T8	495	3.800E+4	13.64	0.725	12.08	0.642
S1T9	495	3.800E+4	15.11	0.804	14.40	0.766
S2T1	485	1.023E+5	32.48	0.655	30.94	0.624
S2T2	485	1.099E+5	38.32	0.719	29.07	0.545
S2T3	485	1.052E+5	45.74	0.897	42.01	0.823
S3T1(R)	529	5.293E+4	22.32	0.797	23.31	0.833
S3T2	529	5.293E+4	25.19	0.900	19.79	0.707
S3T3	529	5.293E+4	24.96	0.891	24.65	0.880
S3T4	518	5.395E+4	19.12	0.684	19.79	0.708
S3T5	518	5.395E+4	26.57	0.951	18.95	0.678
S3T6	518	5.395E+4	23.92	0.856	24.46	0.875
S7T1	527	2.687E+4	11.77	0.831	11.29	0.868
S7T2	548	2.672E+4	11.29	0.771	11.75	0.803
S7T3	512	2.745E+4	10.26	0.730	8.78	0.625
S7T5	510	2.749E+4	11.50	0.820	11.43	0.815

Table 6: R-factors Calculated from Non-Linear Analysis

	Fixed End Rotations R_{Fixed}	**Free End Rotations** R_{Free}	**Australian/New Zealand Draft Standard** R
	Simply-Supported & 3-Span Continuous		
No Bridging	0.77	0.79	0.75
One Row	0.79	0.66	0.85
Two Rows	0.84	0.83	1.00
	2-Span Continuous		
No Bridging	0.65	0.62	0.60
One Row	0.72	0.55	0.70
Two Rows	0.90	0.82	0.80

Table 7: Comparison of R-factors for Simple Purlins

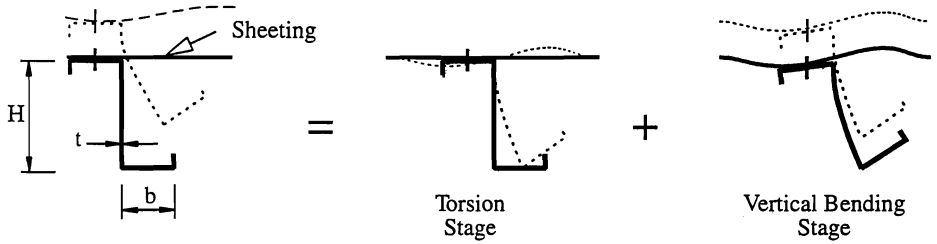

(a) Deformation of a Z-Section

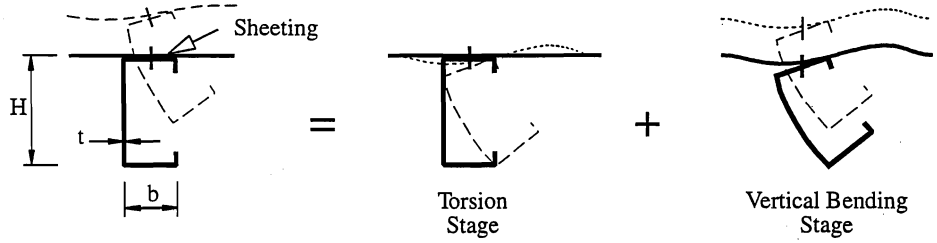

(b) Deformation of a Channel

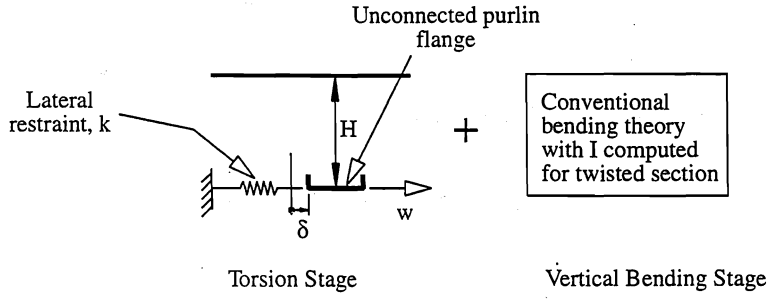

(c) Beam Column Model

Fig.1 Peköz and Soroushian Distorted Section Model

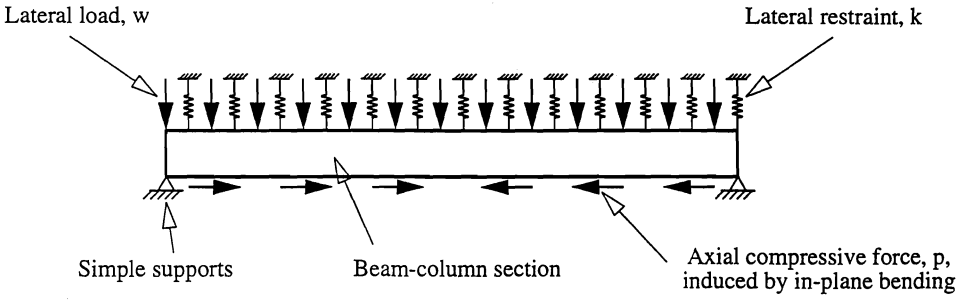

(a) Idealised Beam-Column Section

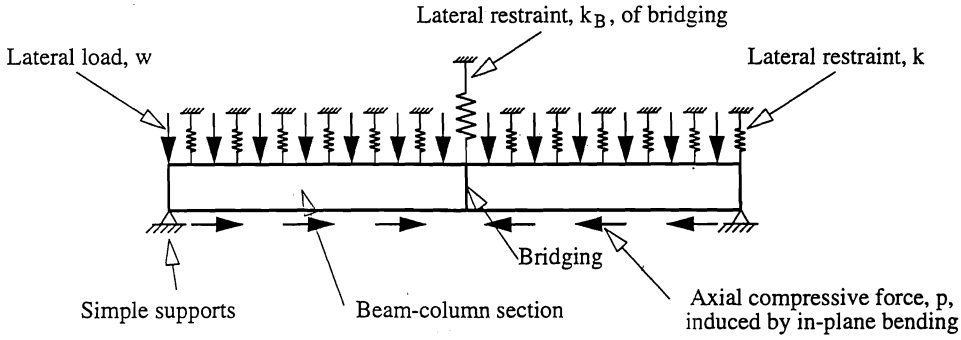

(b) Idealised Beam-Column Section for Purlin with Bridging

Fig.2 Simply-Supported Purlin Model

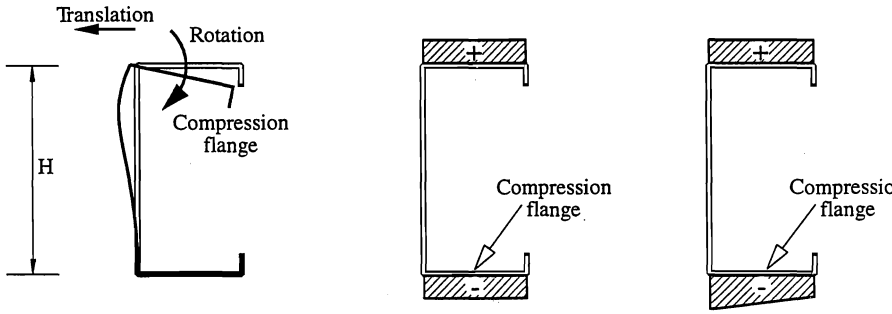

(a) Buckling Mode (b) Assumed Stress Distribution in Flanges (c) Actual Stress Distribution in Flanges

Fig.3 Distortional Buckling of Channel Purlin

NF - Narrow Flange connected

WF - Wide Flange connected

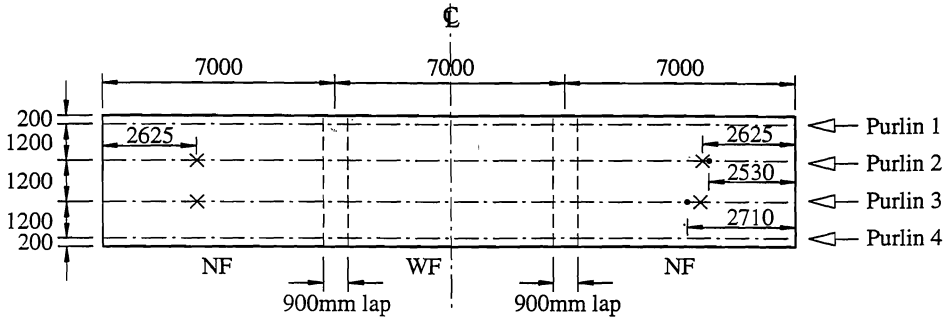

(a) Test 1

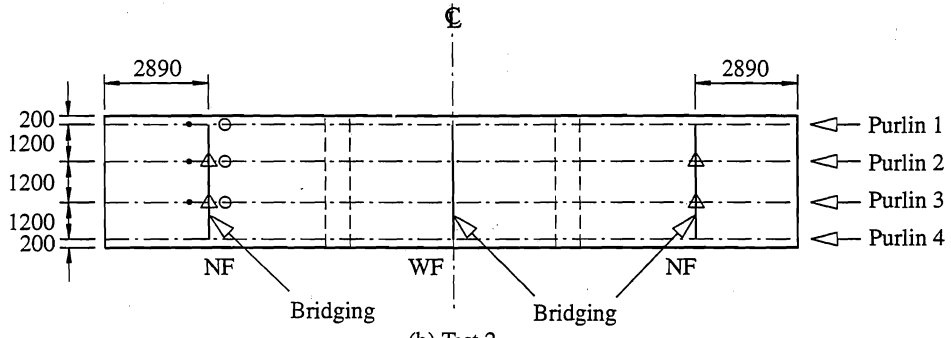

(b) Test 2

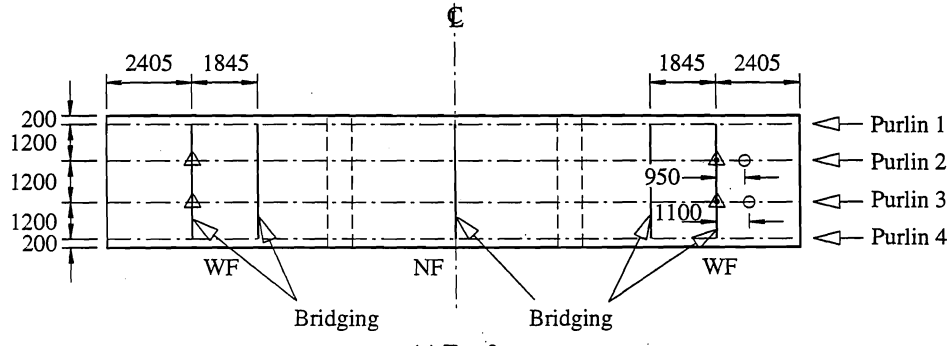

(c) Test 3

Legend:

- • Flange-web local buckle - test
- × Flange-web local buckle - analysis
- (all dimensions in mm)
- ○ Lip stiffener buckle - test
- ■ Outer flange failure - test
- △ Distortional buckle - analysis

Fig.4 Series 1 - Z15019

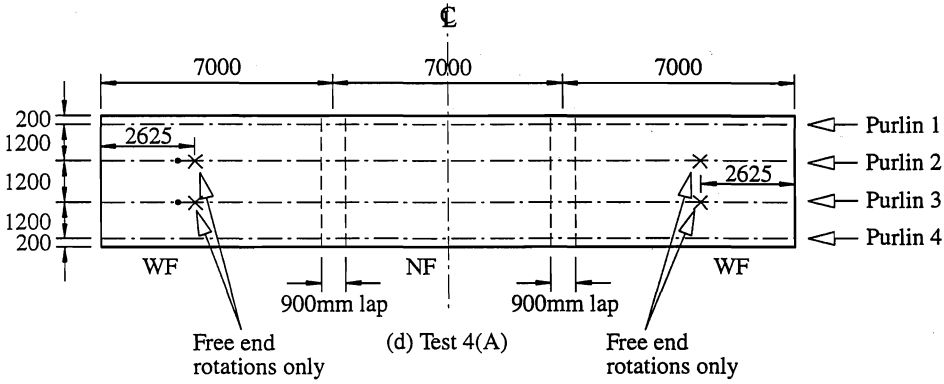

(d) Test 4(A)

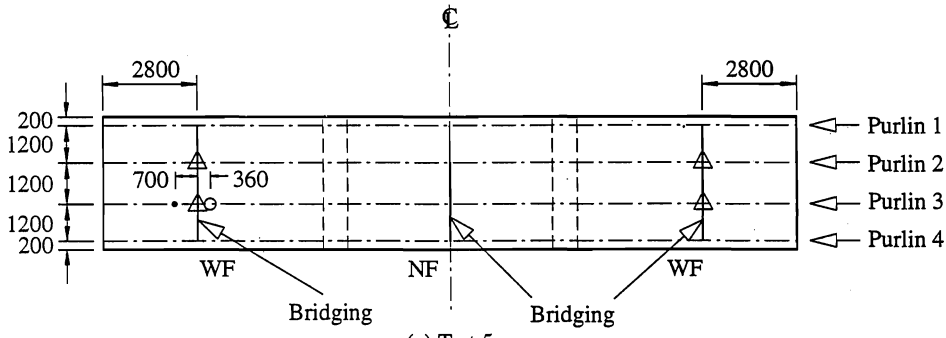

(e) Test 5

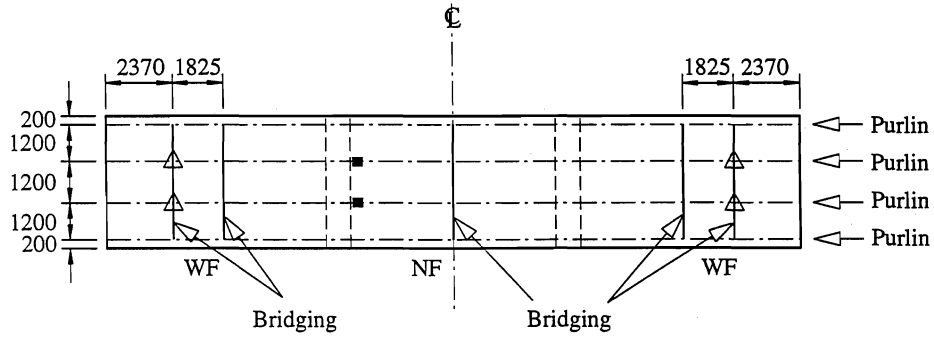

(f) Test 6

Legend:

- • Flange-web local buckle - test
- × Flange-web local buckle - analysis
- o Lip stiffener buckle - test
- ■ Outer flange failure - test
- △ Distortional buckle - analysis

(all dimensions in mm)

Fig.4 Series 1 - Z20015

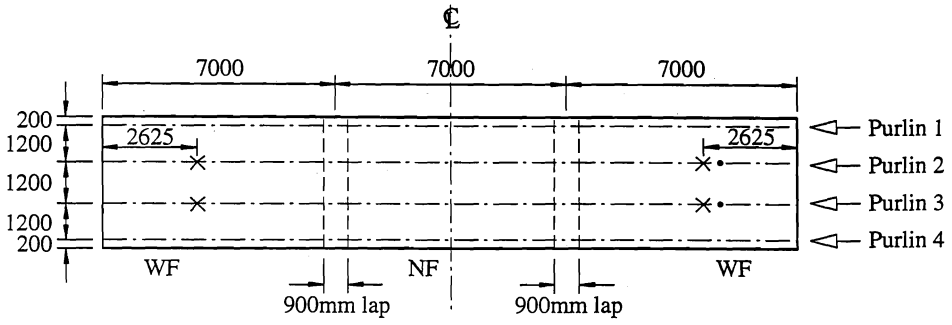

(g) Test 7

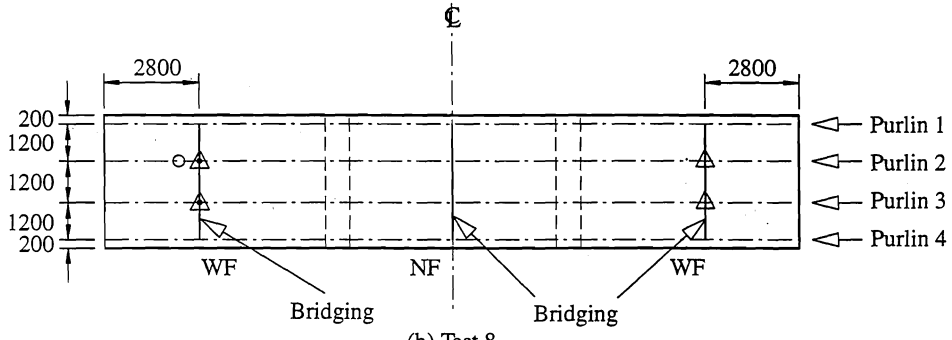

(h) Test 8

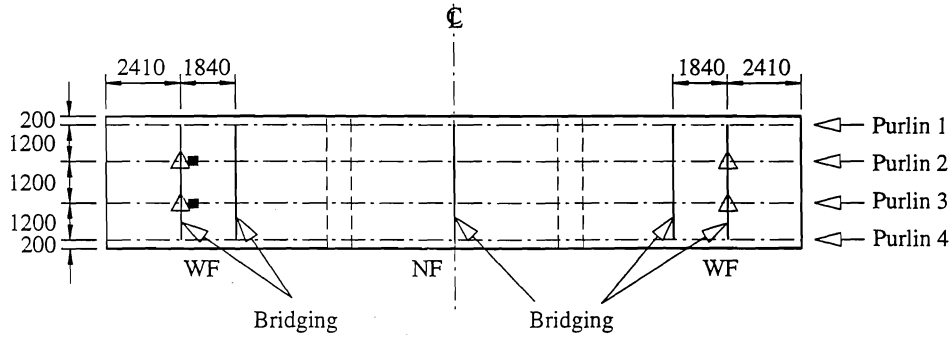

(i) Test 9

Legend:

- • Flange-web local buckle - test
- × Flange-web local buckle - analysis
- (all dimensions in mm)
- ○ Lip stiffener buckle - test
- ■ Outer flange failure - test
- △ Distortional buckle - analysis

Fig.4 Series 1 - Z20019

NF - Narrow Flange connected
WF - Wide Flange connected

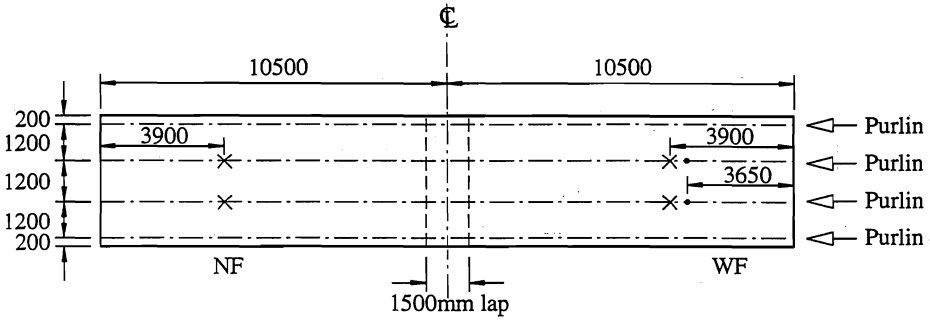

(a) Test 1

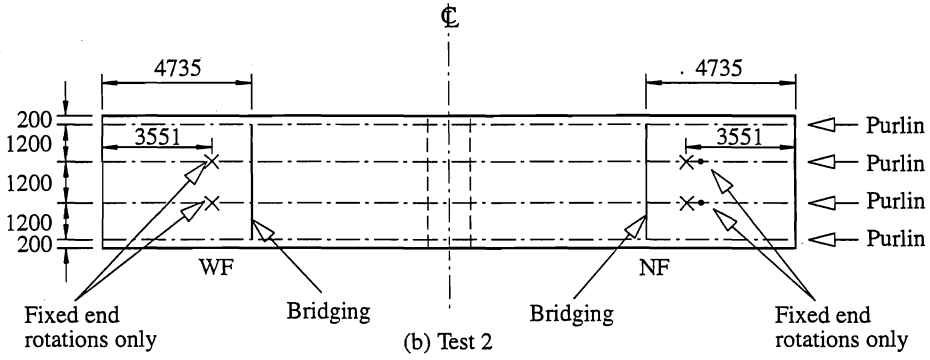

(b) Test 2

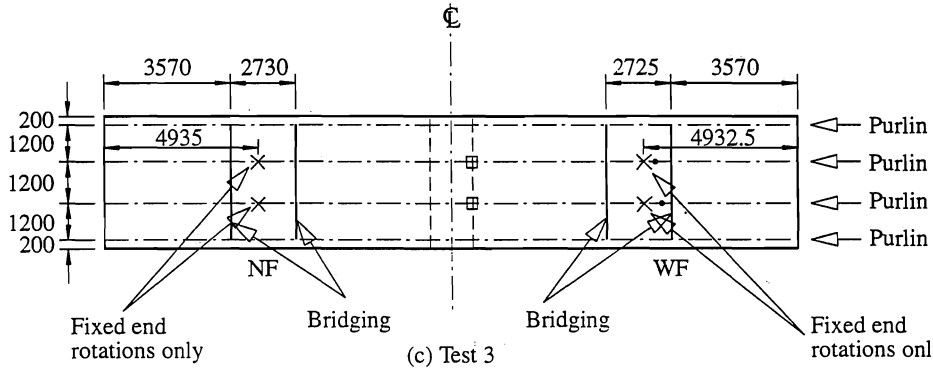

(c) Test 3

Legend:

- • Flange-web local buckle - test
- × Flange-web local buckle - analysis
- □ Inner flange failure-test
- △ Distortional buckle-analysis

(all dimensions in mm)

Fig.5 Series 2 - Z30025

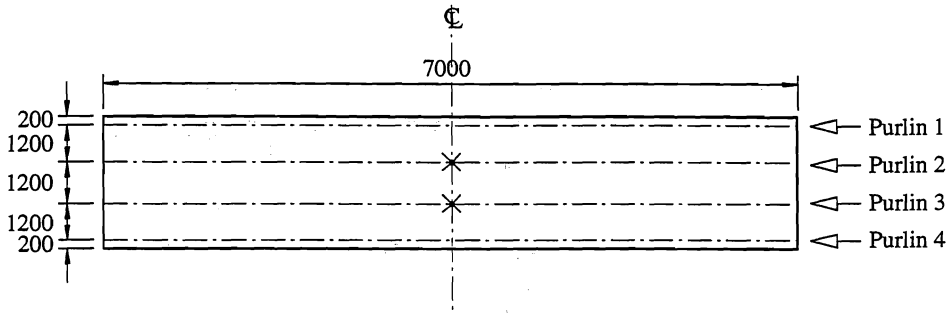

(a) Test 1 (R)

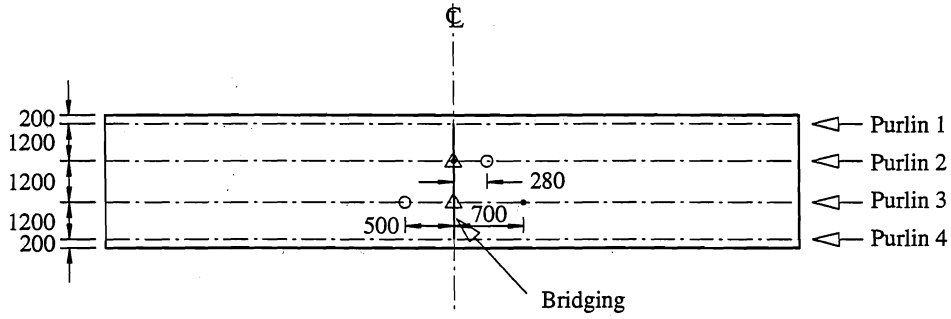

(b) Test 2

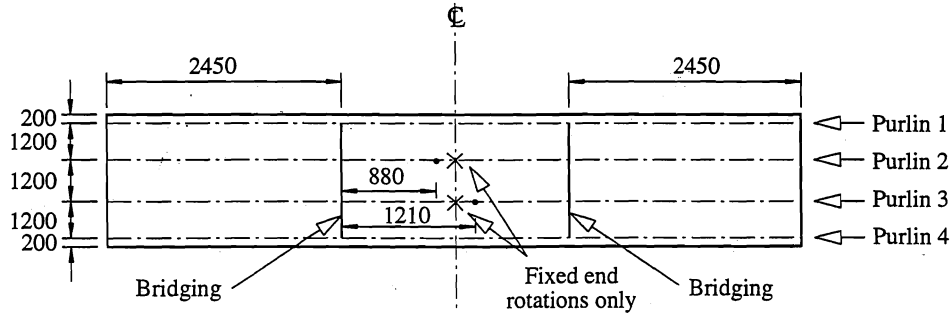

(c) Test 3

Legend:

- • Flange-web local buckle - test
- × Flange-web local buckle - analysis
- (all dimensions in mm)
- ○ Lip stiffener buckle - test
- ■ Outer flange failure - test
- △ Distortional buckle - analysis

Fig.6 Series 3 - Z20024

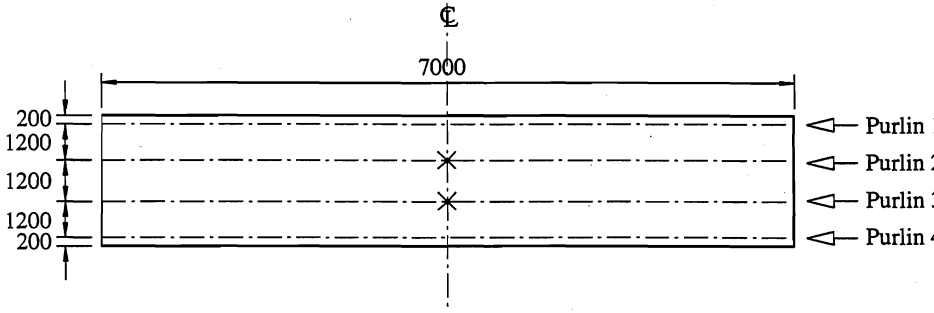

(d) Test 4

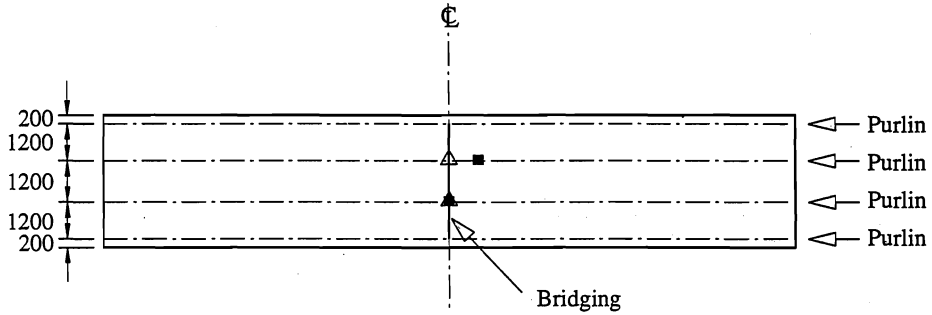

(e) Test 5

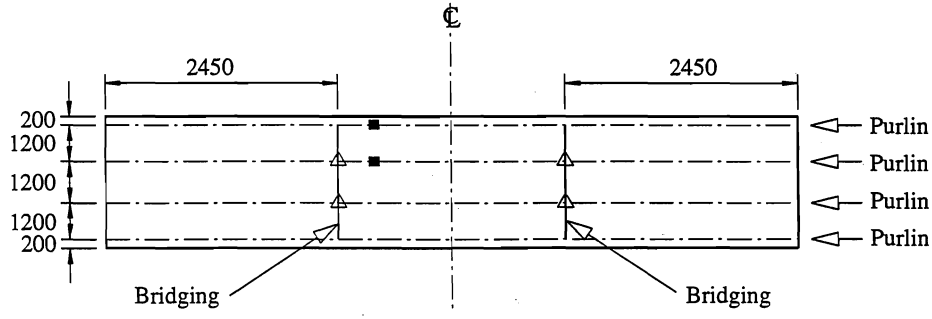

(f) Test 6

Legend:

- • Flange-web local buckle - test
- × Flange-web local buckle - analysis
- (all dimensions in mm)
- o Lip stiffener buckle - test
- ■ Outer flange failure - test
- △ Distortional buckle - analysis

Fig.6 Series 3 - C20024

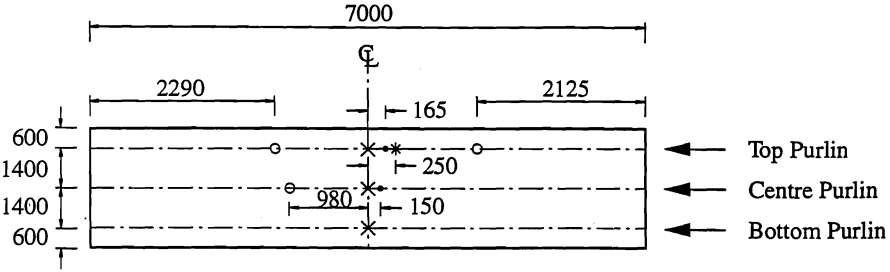

(a) Test 1 - Z20015

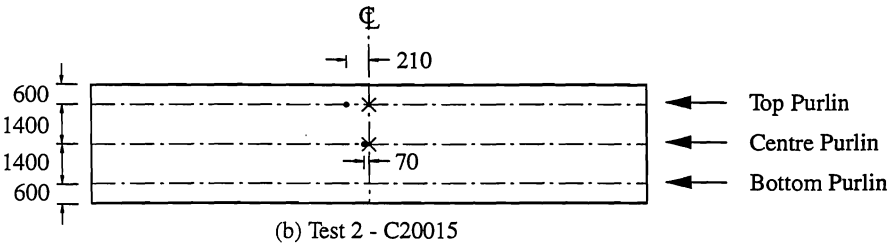

(b) Test 2 - C20015

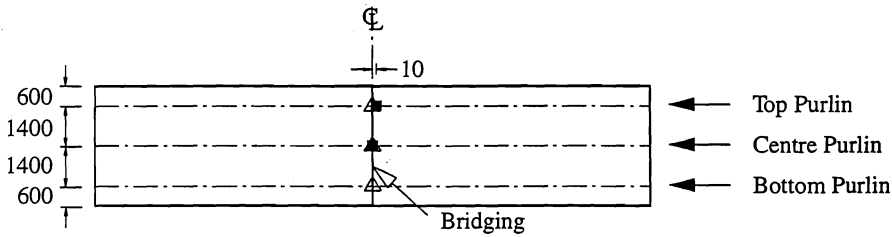

(c) Test 3 - C20015

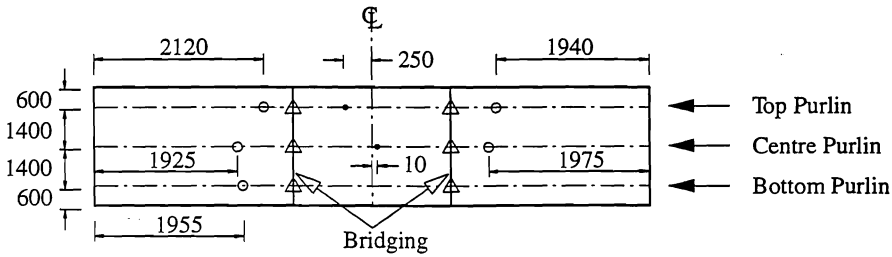

(d) Test 5 - C20015

- • Flange-web local buckle-test
- × Flange-web local buckle-anlysis
- ○ Lip stiffener buckle-test
- ✳ Lip stiffener buckle, inner flange-test
- ■ Outer flange failure-test
- △ Distortional buckle-analysis

(all dimensions in mm)

Fig.7 Series 7